Quantum particle in a washboard potential. II. Nonlinear mobility and the Josephson junction

Yong-Cong Chen* and Joel L. Lebowitz
Department of Mathematics and Physics, Rutgers Universtiy, New Brunswick, New Jersey 08903
(Received 19 February 1992; revised manuscript received 19 June 1992)

We obtain an analytic expression for the nonlinear mobility of a quantum particle moving down a cosine potential in the presence of a finite bias force in the small viscosity limit. This is used to explain some experimental observations in Josephson junctions in which the Coulomb blockade is important. The result is based on a resummation of a series expansion of the mobility in V_0 (the strength of the cosine potential) and is applicable to a variety of regimes in the parameter space.

I. INTRODUCTION

This paper is part of an investigation of the dynamics of a quantum particle moving in a periodic cosine potential while coupled to a boson bath.[1-3] Our analysis uses a real-time Wigner distribution function formalism. Due to the direct relation between the velocity of the particle, v_F, under an external driving force, F, and the I-V characteristic of a current-biased Josephson junction ($I \leftrightarrow F$, $V \leftrightarrow v_F$), this problem has attracted a great deal of theoretical interest;[4-9] cf. the accompanying paper[3] (hereafter referred to as I) for background. Our starting point here is the formally exact series expansion for v_F in terms of V_0, the strength of the cosine potential (cf. Sec. IV of I) and our interest is in the small viscosity limit of an Ohmic dissipation, $J(\omega)=\eta\omega$.

This case is relevant to realistic experiments involving quantum effects in ultrasmall Josephson tunnel junctions. In general the presence of hysteretic I-V curves, which appears only when the viscosity is below a certain value, is essential in macroscopic quantum tunneling measurements.[6] Note, however, that the small viscosity limit is by no means an indication of weak effects of dissipation on the quantum dynamics of the particle. On the contrary, the effects are expected to be important for the mobility since the particle is eventually stopped at rather large velocities by the dissipation.

The strategy used here is to first divide the multidimensional time integrals which appear as coefficients in the series expansion into "neutral charge" clusters (viewing each time argument t_j of the integrands as the position of a particle with charge μ_j). In each cluster the total charge is zero. When the viscosity is small, the links between clusters are in general very weak so that they are well separated from each other. For a given cluster, we employ again the weak damping limits of the various functions entering the integrands. This enables us to carry out the intracluster integration exactly and transform the series for the mobility into an expansion in the neutral charge clusters (or equivalently in $1/\eta$, the inverse of the viscosity). We then find that the new expansion can be represented by an integral equation which can be solved via self-consistency. This leads to an analytic expression for v_F as a function of $\tilde{F}=F/\eta$ which is expected to describe the small viscosity limit of the dynamics in almost the entire parameter space. The result shows in particular the effects of the quantum Bloch states on the particle's dynamics. The striking feature is that this was not an explicit input for the computation at the starting point. We then compare our results with experimental observations in ultrasmall Josephson junctions[7] where quantum effects, the so-called Coulomb blockade, are important. It seems to provide a reasonably satisfactory explanation for the various experimental phenomena.

The plan of this paper is as follows. In Sec. II we review briefly the general expression for the stationary velocity v_F as a series in V_0. Then in Sec. III we discuss the concept of the neutral charge cluster and deal with the problem of summing over a single irreducible cluster. The method is generalized in Sec. IV to include multicluster terms. We then sum over the entire series in the cluster expansion to get the analytic expression for the quantum mobility. In Sec. V we present plots of v_F vs $\tilde{F}$ for various parameters and discuss the relation of our result to the experimental observations in small Josephson junctions.

II. THE STATIONARY VELOCITY

We consider a system with Hamiltonian

$$\hat{H}_p=\frac{\hat{p}^2}{2m}+V_0\cos(k_0\hat{x})-Fx \tag{1}$$

coupled to a boson bath with an Ohmic dissipation spectrum $J(\omega)=\eta\omega$. Starting with an initial product density matrix for the bath in equilibrium and the system localized at the origin, one finds for v_F, the mean velocity of the particle subject to a force F, see I,

$$v_F=\lim_{t\to\infty}\frac{\langle\hat{x}\rangle(t,F)}{t}\ , \tag{2}$$

the series,

$$v_F=\frac{F}{\eta}+\frac{k_0}{2\eta}\sum_{n=1}^{\infty}(-1)^n V_0^{2n}\int_{-\infty}^{0}dt_{2n-1}\cdots\int_{-\infty}^{t_2}dt_1\sum_{\{\mu_j=\pm1\}}(-1)\exp\left[i\frac{Fk_0}{\eta}\sum_{k=1}^{2n}\mu_k t_k\right]F_1F_2\Big|_{t_{2n}=\sum_{j=1}^{2n}\mu_j=0}\ . \tag{3}$$

The functions F_1 and F_2 entering (3) are

$$F_1(\{t_j,\mu_j\})=\sum_{k=1}^{2n-1}\frac{1}{\hbar}\sin\left[\frac{k_0^2}{2}\sum_{j=k+1}^{2n}\mu_j g(t_j-t_k)\right], \tag{4}$$

$$F_2(\{t_j,\mu_j\})=\exp\left[\frac{k_0^2}{2}\sum_{k,k=1}^{2n}\mu_j\mu_k C(t_j-t_k)\right], \tag{5}$$

where

$$g(t)=\frac{\theta(t)}{\eta}[1-\exp(-\eta t/m)] \tag{6}$$

and

$$C(t)=\int_{-\infty}^{\infty}\frac{d\omega}{2\pi}\frac{\hbar\eta\omega}{m^2\omega^4+\eta^2\omega^2}[1-\cos\omega t]\coth\frac{\beta\hbar\omega}{2}$$
$$=\frac{1}{\eta}kT[|t|-mg(|t|)]+O(\eta)\,. \tag{7}$$

Identical expressions for the velocity have been obtained in Ref. 2 (and references therein). Note that the expression for the corresponding tight-binding model,[4] though appearing similar in structure, is actually different from ours in detail (mathematically the tight-binding model seems to correspond roughly to $m\to 0$ and $\eta\to 1/\eta$ of the continuous model).

III. EXPANSION IN NEUTRAL CHARGE CLUSTERS

A. The neutral charge clusters

The coefficients of V_0 in (3) consist of multidimensional integrals over past times. It is useful to divide $\{t_1,t_2,\ldots,t_{2n-1},t_{2n}\}$ into irreducible neutral charge clusters according to their "charges" $\{\mu_j\}$. Here we have made an analogue of the integrals with a one-dimensional Coulomb system, viewing each t_j as the position of a particle carrying charge μ_j. The particles cannot cross over each other. Let the cluster α have a length $2L_\alpha$ and start with $j=J_\alpha$; it terminates at $j=J'_\alpha=J_\alpha+2L_\alpha$. The number of irreducible clusters depends on the distribution of $\{\mu_j\}$. Given a set of $\{\mu_j\}$, we then have

$$\{t_1,t_2,\ldots,t_{2n-1},t_{2n}\}$$
$$\to\{\{t_{j(1)}\},\{t_{j(2)}\},\ldots,\{t_{j(\alpha)}\},\ldots\}$$

with

$$\sum_{j_{(\alpha)}=J_\alpha}^{J'_\alpha}\mu_{j_{(\alpha)}}=0\,,\quad \alpha=1,2,\ldots\,.$$

One then finds that large distances for intracluster "charges" are exponentially suppressed by the function $F_2(\{t_j,\mu_j\})$. To see this let us put, for example, one charged particle, say t_p, far away from its cluster centered at $t=t_c$. Since $C(t)\cong kT|t|/\eta$ at large t the integrand is suppressed by an exponentially decaying factor $\sim\exp(-k_0^2|t_c-t_p|kT/\eta)$. This mechanism does not work for intercluster separations. In the latter case the suppressions come from the function $F_1(\{t_j,\mu_j\})$. Since the clusters are charge neutral, the suppression for the connection between the αth and $(\alpha-1)$th clusters becomes

$$\sin\left[\frac{\hbar k_0^2}{2}\sum_{j=J_\alpha}^{2n-1}\mu_j g(t_j-t_{J'_{\alpha-1}})\right]\sim\sin\left[\frac{\hbar k_0^2}{2}\sum_{j_{(\alpha)}}\mu_{j_{(\alpha)}}g(t_{j_{(\alpha)}}-t_{J'_{\alpha-1}})\right]$$
$$\sim-\frac{\hbar k_0^2}{2}\frac{\partial}{\partial t_{J'_{\alpha-1}}}g(t_{J_\alpha}-t_{J'_{\alpha-1}})\sum_{j_{(\alpha)}}t_{j_{(\alpha)}}\mu_{j_{(\alpha)}}$$
$$\sim-\frac{\hbar k_0^2}{2}\exp[-\eta(t_{J_\alpha}-t_{J'_{\alpha-1}})/m]\sum_{j_{(\alpha)}}t_{j_{(\alpha)}}\mu_{j_{(\alpha)}}\,, \tag{8}$$

which converges for integration over $t_{J'_\alpha}$. Note that if the viscosity η is small, the right-hand side of (8) decays very slowly so that the intercluster separations are typically very large.

B. The small viscosity limit

It is now crucial to notice that the size of a neutral charge cluster becomes, on the other hand, nearly independent of the viscosity when the latter is small. In fact, for $\eta\to 0$ the limits of $g(t)$ and $C(t)$ entering (4) and (5) can be approximated, for fixed $t\neq 0$ by

$$g(t)=\theta(t)\frac{t}{m}\,,\quad C(t)=\frac{kT}{2m}t^2\,. \tag{9}$$

These quantities have the property that the analytic continuation of $R(t)=k_0^2[i\hbar g(t)/2+C(t)]$ satisfies $R(t-i\beta\hbar)=R^*(t)$, an analyticity essential for the validity of the Einstein relation; see Sec. IV A of I. For $t\to 0$ a quantum correction comes in, giving an asymptotic behavior of $C(t)$ of the form $C(t)\sim\eta t^2\ln\beta\hbar/t$, cf. also Ref. 5. This correction can, however, be quite safely ignored as η is small here. For a given neutral charge cluster one can further rewrite

$$\exp\left[\frac{k_0^2}{2}\sum_{j,k=1}^{2L}\mu_j\mu_k C(t_k-t_j)\right]=\exp\left[\frac{k_0^2 kT}{4m}\sum_{j,k=1}^{2L}\mu_j\mu_k(t_j-t_k)^2\right]$$
$$=\sqrt{m/2\pi k_0^2 kT}\int_{\infty}^{-\infty}d\xi\exp\left[-\frac{m}{2k_0^2 kT}\xi^2-i\xi\sum_{j=1}^{2L}\mu_j t_j\right], \tag{10}$$

which enables us to conveniently evaluate intracluster integrals exactly. Our strategy then is to rearrange the series (3) for the stationary velocity v_F into a new one in terms of the neutral charge clusters; the nth order will then involve n clusters with complicated interactions between them. Since the interactions decay as $\exp(-\eta t/m)$, this becomes an expansion in $1/\eta$ upon integrations over the intercluster separations. It is evident that an efficient method for summation over all the clusters is essential in order to understand the behavior of the dynamics in this limit. In what follows we shall first work out step by step the whole structure of the series and show that the resummation can be reduced to solving an integral equation.

C. Summing over an irreducible cluster

We first consider the summation over V_0 for a single irreducible cluster. Although the result is just the first-order term in the new expansion in $1/\eta$, it is an essential step to understand the whole structure of the series. To proceed let us associate to the integrands an exponential decay factor of the form $\exp(\epsilon t_1)$, $\epsilon\to 0^+$; this is necessary when one uses (10). Furthermore, let us scale at this point all relevant quantities to be dimensionless with respect to the system's intrinsic parameters m, k_0, and V_0,

$$\frac{F}{k_0 V_0}\to F\ ,\quad \frac{kT}{V_0}\to T\ ,$$
$$\frac{\eta}{\sqrt{mk_0^2 V_0}}\to\eta\ ,\quad \frac{\hbar k_0}{2\sqrt{mV_0}}\to\Omega_q\ , \tag{11}$$

where Ω_q is the dimensionless form of $\hbar k_0^2/2m$ (a measure of quantum effects in frequency). All velocities and times are hereafter measured in units of $\sqrt{V_0/m}$ and $(k_0\sqrt{V_0/m})^{-1}$, respectively. Carrying out the integration over the different t's yields the velocity due to the irreducible cluster,

$$v_{(1)}(\tilde{F},T)=\frac{1}{2\eta}\sum_{L=1}^{\infty}\frac{(-1)^L}{(2\Omega_q)^{2L-1}}f_L\ , \tag{12}$$

where

$$\tilde{F}\equiv F/\eta\ , \tag{13}$$

$$f_L=\frac{-i}{\sqrt{2\pi T}}\int_{-\infty}^{\infty}d\xi\exp\left[-\frac{\xi^2}{2T}\right]\sum_{\{\mu_j,\sigma_j=\pm1\}}\prod_{k=1}^{2L-1}\frac{-i\sigma_k/2}{i\left[\sum_{j=1}^{k}\mu_j\right]\left[\tilde{F}-\xi+\Omega_q\sum_{j=1}^{k}\sigma_j\right]+\epsilon}\ . \tag{14}$$

The poles of integrands are on the two sides of the real axis. If we close the integral over ξ in the upper half plane, only the poles above the real axis are picked up. However, integration along any contour a finite distance off the real axis simply vanishes since for $\epsilon\to 0$ the integrand is odd under $\mu_j\to-\mu_j$. Therefore we have

$$f_L=\frac{A_L}{\sqrt{2\pi T}}\oint d\xi\exp\left[-\frac{\xi^2}{2T}\right](-1)$$
$$\times\sum_{\{\sigma_j=\pm1\}}\prod_{k=1}^{2L-1}\frac{\sigma_k/2}{\tilde{F}-\xi+\Omega_q\sum_{j=1}^{k}\sigma_j}\ , \tag{15}$$

where the contour of the integration encloses the poles of the integrand and

$$A_L=\sum_{\{\mu_j\}}\frac{\mu_{2L}}{2}\prod_{k=1}^{2L-1}\left[\sum_{j=1}^{k}\mu_j\right]^{-1} \tag{16}$$

is just a numerical factor with the summation restricted to the irreducible neutral charge cluster of length $2L$.

The evaluation of A_L for large L is difficult. One can think of A_L as the partition function of a one-dimensional lattice system of size $2L$. As L becomes large, one expects that the boundary effects will be negligible and that $A_L^{1/(2L-2)}$ will exist as $L\to\infty$. In fact, the approximation $A_L\cong Z^{2L-2}$ is excellent for $Z\simeq 0.8$. The differences between $A_L^{1/(2L-2)}$ and Z are negligible for all

L (with the exception of the lowest one $L=2$ which has $A_2^{1/2}\cong 0.71$, but this can be easily fixed when this term is dominant). It remains to calculate the residues of the integrands, some of which are from higher-order poles.

It is illustrative to consider first the so-called classical limit where $\hbar\to 0$, i.e., the dimensionless $\Omega_q\to 0$. In this case the summation over the σ_j's reduces to taking derivatives with respect to ξ. We thus have

$$f_L = i\frac{A_L}{\sqrt{2\pi T}}\oint d\xi\,\Omega_q^{2L-1}\exp\left[-\frac{\xi^2}{2T}\right]\left[\frac{d}{d\xi}\frac{1}{\tilde F-\xi}\right]^{2L-1}$$

$$= -\sqrt{2\pi/T}\,A_L\frac{\partial}{\partial\tilde F}\frac{\Omega_q^{2L-1}}{2^{2L-2}(2L-2)!}\left[\left[\frac{\partial}{\partial\tilde F}\right]^2\right]^{2L-2}\exp\left[-\frac{\tilde F^2}{2T}\right]. \tag{17}$$

Now the series expansion (12) for $v_{(1)}$ can be readily summed up. It yields

$$v_{(1)}(\tilde F,T)|_{\Omega_q\to 0} = \frac{1}{4\eta}\sqrt{2\pi/T}\cos\left[\frac{Z}{4}\left[\frac{\partial}{\partial\tilde F}\right]^2\right]\frac{\partial}{\partial\tilde F}\exp\left[\frac{\tilde F^2}{2T}\right]. \tag{18}$$

The derivatives in (18) can actually be carried out by means of Fourier transforms. We obtain

$$v_{(1)}|_{\Omega_q\to 0} = \frac{\sqrt{2\pi}}{8\eta}\frac{\partial}{\partial\tilde F}\sum_{\sigma=\pm 1}[T+i\sigma Z/2]^{-1/2}\exp\left[-\frac{\tilde F^2}{2(T+i\sigma Z/2)}\right]. \tag{19}$$

In the "quantum" case, i.e., Ω_q finite, we have to deal with the evaluation of many residues arising from the poles near $\xi=\tilde F$; they are spread around $\xi=\tilde F$ in a band of width Ω_q. At first sight, it seems rather difficult to compute the general terms because higher-order poles also play a role. Fortunately, the problem can be solved based on the following observations: First of all, a detailed term by term analysis of the symmetry structure of (15) reveals that terms containing derivatives of $\exp(-\xi^2/2T)$ completely cancel. Thus for the Lth-order term the result of the loop integration over ξ can be written as

$$f_L = -\sqrt{2\pi/T}\frac{A_L}{\Omega_q^{2L-2}}\sum_{l=-2L+1}^{2L-1} w_l\exp\left[-\frac{(\tilde F-l\Omega_q)^2}{2T}\right]. \tag{20}$$

One also finds that f_L is odd under $\Omega_q\to-\Omega_q$, so that $w_l=-w_{-l}$. Finally, one realizes that the limit $\Omega_q\to 0$ must coincide with the corresponding classical limit, i.e., Eq. (17). This shows that the right-hand side of (20) is proportional to the lattice version of the $(4L-3)$th-order derivative of $\exp(-\tilde F^2/2T)$. The derivative requires at least $(4L-2)$ lattice points. Since we also require, in addition, the odd symmetry under $\Omega_q\to-\Omega_q$, it turns out that w_l is uniquely determined. The result is

$$f_L = -\frac{A_L\sqrt{2\pi/T}}{2^{2L-2}(2L-2)!\Omega_q^{2L-2}}\{\tfrac{1}{2}[(\hat d_\xi^+-1)^{4L-3}(\hat d_\xi^-)^{2L-2}-(\hat d_\xi^--1)^{4L-3}(\hat d_\xi^+)^{2L-2}]\exp[-\xi^2/2T]\}|_{\xi=\tilde F}, \tag{21}$$

where we have introduced a set of "lattice" displacement operators

$$\hat d_\xi^+\phi(\xi)=\phi(\xi+\Omega_q),\quad \hat d_\xi^-\phi(\xi)=\phi(\xi-\Omega_q). \tag{22}$$

The summation over the infinite series can again be handled by Fourier transform; we have

$$f_L = -\frac{A_L}{2^{2L-2}(2L-2)!\Omega_q^{2L-2}}\int_{-\infty}^{\infty}dp\frac{i\sin p\Omega_q}{\Omega_q}\left[2\sin\frac{p\Omega_q}{2}\right]^{4L-4}\exp\left[ip\tilde F-\frac{Tp^2}{2}\right]. \tag{23}$$

Substituting this back to (12) we then obtain

$$v_{(1)}(\tilde F,T) = \frac{1}{4\eta}\int_{-\infty}^{\infty}dp\frac{i\sin p\Omega_q}{\Omega_q}\cos\left[\frac{Z}{4\Omega_q^2}\left[2\sin\frac{p\Omega_q}{2}\right]^2\right]\exp\left[ip\tilde F-\frac{Tp^2}{2}\right]. \tag{24}$$

Clearly it matches the classical limit as $\Omega_q\to 0$. The result of (24) is valid for arbitrary Ω_q except in the extreme case where only the first few (1 or 2) orders dominate the series. In the latter case one can simply take the exact value of A_L and cut the series at some convenient $L_{\max}$.

IV. SUMMING OVER THE NEUTRAL CLUSTERS

A. Two-cluster problem

We now study the interactions between clusters. Let us start with a two-cluster problem; the result will then be generalized to higher orders in the cluster expansion. In the small viscosity limit the distance $\tau_2-\tau_1=\tau_{21}$ between the lower cluster (cluster 1) and the upper cluster (cluster 2) is of the order $1/\eta$, which is much larger than the intracluster distances of the order $T^{-1/2}$. Returning to (3)–(5), the relevant functions connecting the two parts behave as

$$\sum_{j_{(2)}} \mu_{j_{(2)}} g(t_{j_{(2)}}-t_{j_{(1)}})=\exp(-\eta\tau_{21}) \sum_{j_{(2)}} \mu_{j_{(2)}} t_{j_{(2)}}+O(\eta) \tag{25}$$

and

$$\sum_{j_{(1)},j_{(2)}} \mu_{j_{(1)}}\mu_{j_{(2)}} C(t_{j_{(1)}}-t_{j_{(2)}})=-T\left[\sum_{j_{(1)}} t_{j_{(1)}}\right]\exp(-\eta\tau_{21})\left[\sum_{j_{(2)}} \mu_{j_{(2)}} t_{j_{(2)}}\right]+O(\eta)\ . \tag{26}$$

Using (25) and (26), it is now straightforward to integrate over the internal degrees of the two clusters while fixing τ_{21}. In doing this we have implicitly neglected the sizes of the clusters with respect to the distance between them. The procedure is similar to that performed for the single-cluster problem. The two-cluster contribution to v_F [see (3)] can be approximated by [let $g\equiv\exp(-\eta\tau_{21})$]

$$\begin{aligned} v_{(2)}=\frac{(-i)}{2\eta^2}\sum_{L_2,L_1=1}^{\infty}\int_0^1\frac{dg}{g}\Bigg\{&\frac{Z^{2(L_2+L_1)-4}(-1)^{L_1+L_2}}{(2\Omega_q)^{2(L_2+L_1)-1}}\sum_{\{\sigma_j^{(1)},\sigma_j^{(2)}=\pm1\}}\oint\frac{d\xi_1}{\sqrt{2\pi T}}\exp\left[-\frac{\xi_1^2}{2T}\right] \\ &\times\left[\prod_{k=1}^{2L_1-1}\frac{-\sigma_k^{(1)}/2}{\tilde F-\xi_1-\Omega_q\sum_{j=1}^{k}\sigma_j^{(1)}}\right]\frac{(+i\sigma_{2L_1}^{(1)})}{2} \\ &\times\oint\frac{d\xi_2}{\sqrt{2\pi T(1-g^2)}}\exp\left[-\frac{\xi_2^2}{2T(1-g^2)}\right]\prod_{k=1}^{2L_2-1}\frac{-\sigma_k^{(2)}/2}{\tilde F-g\xi_1-\xi_2-\Omega_q\left[g\sum_{j=1}^{2L_1}\sigma_j^{(1)}+\sum_{j=1}^{k}\sigma_j^{(2)}\right]}\Bigg\}\ . \end{aligned} \tag{27}$$

The integral over ξ_2 and summation over L_2 can be readily carried out. This leads to

$$\begin{aligned} v_{(2)}=\frac{(-i)}{2\eta}\sum_{L_1=1}^{\infty}\frac{(-1)^{L_1}Z^{2L_1-2}}{(2\Omega_q)^{2L_1-1}}\int_0^1\frac{dg}{g}\Bigg\{&\oint\frac{d\xi_1}{\sqrt{2\pi T}}\exp\left[-\frac{\xi_1^2}{2T}\right]\sum_{\{\sigma_j^{(1)}=\pm1\}}\left[\prod_{k=1}^{2L_1-1}\frac{-\sigma_k^{(1)}/2}{\tilde F-\xi_1-\Omega_q\sum_{j=1}^{k}\sigma_j^{(1)}}\right] \\ &\times\frac{-\sigma_{2L_1}^{(1)}}{2\Omega_q}v_{(1)}\left[\tilde F-g\left[\Omega_q\left[\sum_{j=1}^{2L_1}\sigma_j^{(1)}\right]+\xi_1\right],T(1-g^2)\right]\Bigg\}\ . \end{aligned} \tag{28}$$

Now again in the classical limit $\Omega_q\to0$ summing over $\sigma_j^{(1)}$ reduces to taking derivatives on ξ_1,

$$\begin{aligned} v_{(2)}=\frac{(-i)}{4\eta}\sum_{L_1=1}^{\infty}(-1)^{L_1}\left[\frac{Z}{2}\right]^{2L_1-2}\int_0^1\frac{dg}{g}\oint\frac{d\xi_1}{\sqrt{2\pi T}}\exp\left[-\frac{\xi_1^2}{2T}\right] \\ \times\left[\frac{\partial}{\partial\xi_1}\frac{1}{\tilde F-\xi_1}\right]^{2L_1-1}\frac{\partial}{\partial\xi_1}v_{(1)}(\tilde F-g\xi_1\ ,T(1-g^2))\ . \end{aligned} \tag{29}$$

Expanding $(\partial/\partial\xi_1)v_{(1)}(\tilde F-g\xi_1,T(1-g^2))$ via a Taylor series in $(\tilde F-\xi_1)$, one finds that only even terms play roles in (29). It then yields

$$v_{(2)}=\frac{1}{4\eta}\sum_{L_1>l=0}^{\infty}(-1)^{L_1}\int_0^1\frac{dg}{g}\left\{\left[\frac{\partial}{\partial\xi_1}\left[\left[\frac{Z}{4}\right]\left[\frac{\partial}{\partial\xi_1}\right]^2\right]^{2L_1-2-l}\frac{\sqrt{2\pi/T}}{(2L_1-2-l)!}\exp\left[-\frac{\xi_1^2}{2T}\right]\right]\right.$$
$$\left.\times\left[\frac{(-1)^l}{l!}\frac{\partial}{\partial\xi_1}\left[\left[\frac{Z}{4}\right]\left[\frac{\partial}{\partial\xi_1}\right]^2\right]^l v_{(1)}(\tilde{F}-g\xi_1,T(1-g^2))\right]\right\}\Bigg|_{\xi_1=\tilde{F}}. \tag{30}$$

Following the same reasoning as in the one-cluster problem, in the quantum case the derivatives are replaced by their lattice versions. But the case here is slightly complicated since we have two functions (left-hand side and right-hand side) attached to the integral in different ways. First of all, the argument that no derivatives on the functions (to be discretized) would appear in the expression with finite Ω_q is still valid. However, we have some freedom for a given L_1 to arrange among various lattice derivatives on the left-hand-side or the right-hand-side functions. Suppose that we chose in (30) for a given l the lattice derivatives on the left-hand-side function to be of the form (21) [which now would be a $(4L_1-3-2l)$th-order derivative]. Then it follows that the lattice derivatives on the right-hand-side function can only take the form (21) too. This is based on two observations: (a) the whole term has to be even under $\Omega_q\to-\Omega_q$; (b) from the structure of (28) the maximum displacement on the right-hand-side function allowed is $\pm(l+1)\Omega_q$. Let us now introduce the following sets of operators and functions:

$$\hat{Q}_1(\xi)=\cos\left[\frac{Z}{4}\frac{(d_\xi^+ +d_\xi^- -2)}{\Omega_q^2}\right]\left[\frac{d_\xi^+ -d_\xi^-}{2\Omega_q}\right], \tag{31}$$

$$\hat{Q}_2(\xi)=\sin\left[\frac{Z}{4}\frac{(d_\xi^+ +d_\xi^- -2)}{\Omega_q^2}\right]\left[\frac{d_\xi^+ -d_\xi^-}{2\Omega_q}\right] \tag{32}$$

and

$$y_1(\xi,g)=\hat{Q}_1(\xi)y_0(\xi,g)\ ,\quad y_2(\xi,g)=\hat{Q}_2(\xi)y_0(\xi,g) \tag{33}$$

with

$$y_0(\xi,g)=\frac{1}{4}\left[\frac{2\pi}{T(1-g^2)}\right]^{1/2}\exp\left[-\frac{\xi^2}{2T(1-g^2)}\right]. \tag{34}$$

The result for the two-cluster problem can be written in the form

$$v_{(2)}=-\left[\frac{1}{\eta}\right]\int_0^1\frac{dg}{g}\{[y_1(\tilde{F},0)\hat{Q}_1(\xi)+y_2(\tilde{F},0)\hat{Q}_2(\xi)]v_{(1)}(\tilde{F}-g\xi,T(1-g^2))\}\big|_{\xi=\tilde{F}}. \tag{35}$$

B. Summing over the clusters

We now generalize the method to multicluster terms. The algebra is straightforward but very tedious. The general procedure is as follows. In the first step we go from the bottom to the top with fixed cluster lengths $2L_\alpha$ and intercluster distances $\tau_{(\alpha+1)}-\tau_\alpha=(\ln g_\alpha)/\eta$. We then integrate over the intracluster degrees of freedom of the lowest cluster (cluster 1) by expressing it in terms of a contour integral over ξ_1. It modifies the structures of other clusters. We then integrate over the second lowest one (cluster 2) with the modification from cluster 1. Both will modify the remaining clusters. But the effect of cluster 1 becomes indirect after adding the effect of cluster 2 (cf. below, this is precisely the property that allows us to express the final result in terms of an integral equation). This procedure can be continued until we reach the top. In the second step, we carry out the resulting contour integrals and sum over the series in V_0 for each cluster one by one from the top to the bottom. The final structure turns out to be rather elegant. The $(n+1)$-cluster contribution is

$$v_{(n+1)}=\left[\frac{-1}{\eta}\right]^n\int_0^1\left[\prod_{i=1}^n\frac{dg_i}{g_i}\right]A_n(g_1,g_2,\ldots,g_n). \tag{36}$$

The coefficients can be expressed as

$$A_n=\left\{\left[\sum_{i=1}^2 y_i(\tilde{F},0)\hat{Q}_i(\xi_1)\right]\left\{\left[\sum_{i=1}^2 y_i(\tilde{F}-\xi_1,g_1)\hat{Q}_i(\xi_2)\right]\left\{\cdots\left\{\left[\sum_{i=1}^2 y_i(\tilde{F}-\xi_{n-2},g_{n-2})\hat{Q}_i(\xi_{n-1})\right]\right.\right.\right.$$
$$\left.\left.\left.\times\left\{\left[\sum_{i=1}^2 y_i(\tilde{F}-\xi_{n-1},g_{n-1})\hat{Q}_i(\xi_n)\right]y_1(\tilde{F}-g_n\xi_n,g_n)\right\}\Big|_{\xi_n\to\tilde{F}}\right\}\Big|_{\xi_{n-1}\to\tilde{F}}\cdots\right\}\Big|_{\xi_2\to\tilde{F}}\right\}\Big|_{\xi_1\to\tilde{F}}. \tag{37}$$

Now let us introduce a function $v(\xi,g)$ satisfying the following integral equation:

$$v(\xi,g)=\xi-\left[\frac{1}{\eta}\right]\int_0^1\frac{dg'}{g'}[y_1(\xi,g)\hat{Q}_1(\xi')+y_2(\xi,g)\hat{Q}_2(\xi')]v(\tilde{F}-g'\xi',g')\Big|_{\xi'\to\tilde{F}} . \tag{38}$$

Then summing over all clusters simply gives

$$v_F=\tilde{F}+\sum_{n=0}^{\infty}v_{(n+1)}=v(\tilde{F},g=0) . \tag{39}$$

We have thus reduced the problem of finding the stationary velocity of the particle in the presence of a finite bias to solving the integral equation (38). The equation can be solved via a simple self-consistency requirement. To see this let us rewrite it as

$$v(\xi,g)=\xi-(1/\eta)[y_1(\xi,g)A_1+y_2(\xi,g)A_2] , \tag{40}$$

where

$$A_i=\int_0^1\frac{dg'}{g'}\hat{Q}_i(\xi')v(\tilde{F}-g'\xi',g')\Big|_{\xi'\to\tilde{F}} , \quad i=1,2 \tag{41}$$

are just constants (independent of ξ and g) and thus can be obtained self-consistently. The final result for v_F reads

$$v_F=\tilde{F}+\frac{y_1(\tilde{F},0)(\eta+C_{22})-y_2(\tilde{F},0)C_{21}}{(\eta+C_{11})(\eta+C_{22})-C_{12}C_{21}} , \tag{42}$$

where the coefficients C_{ij} are given by

$$C_{ij}=\left\{\int_0^1\frac{dg}{g}\hat{Q}_i(\xi)\hat{Q}_j(\tilde{F})y_0(\tilde{F}-g\xi,g)\right\}\Big|_{\xi\to\tilde{F}} . \tag{43}$$

The various quantities here may be conveniently evaluated via Fourier transform. We find

$$y_i(\tilde{F},0)=\frac{1}{4}\int_{-\infty}^{\infty}dp\frac{i\sin p\Omega_q}{\Omega_q}S_i\left[\frac{Z}{\Omega_q^2}\left[\sin\frac{p\Omega_q}{2}\right]^2\right]\exp\left[ip\tilde{F}-\frac{Tp^2}{2}\right] \tag{44}$$

and

$$C_{ij}=\frac{1}{4}\int_0^1\frac{dg}{g}\left\{\int_{-\infty}^{\infty}dp\frac{\sin(gp\Omega_q)}{\Omega_q}S_i\left[\frac{Z}{\Omega_q^2}\left[\sin\frac{gp\Omega_q}{2}\right]^2\right]\right.$$
$$\left.\times\frac{\sin(p\Omega_q)}{\Omega_q}S_j\left[\frac{Z}{\Omega_q^2}\left[\sin\frac{p\Omega_q}{2}\right]^2\right]\exp[ip\tilde{F}(1-g)-(1-g^2)Tp^2/2]\right\} . \tag{45}$$

where

$$S_1(x)=\cos x , \quad S_2(x)=\sin x . \tag{46}$$

We emphasize that our result is based on a complete resummation over the formally exact series expansion for v_F and thus is applicable to almost the entire parameter regimes of Ω_q, T, and $\tilde{F}$ in the small viscosity limit (cf. below). Note also that by solving the integral equation we overcome the divergence problem associated with the original series.

We now try to give explicit criteria for the validity of the result (42). Clearly the small viscosity limit requires $T/\eta^2\gg1$. There has been no explicit requirement in the derivation regarding the relative magnitude of Ω_q and η. In the limit $V_0\to0$ where only the leading order in V_0 is kept, it is trivial to show that our result agrees with those of Refs. 2 and 5 when $\eta\to0$. However, including the multicluster terms (which are all higher orders in V_0) leads to a divergence problem for $\Omega_q=0$ (i.e., the pure classical case) as two clusters become close. A short-time cutoff for the intercluster separations may be introduced to remove the divergence. It is not present either as soon as finite Ω_q (i.e., the quantum effect) is introduced. Nevertheless this problem makes further comparisons with the classical result of the Fokker-Planck equation[8] very difficult. In any case, since our main interest lies in the quantum regimes we may as well propose a second criterion for the validity, $\Omega_q/\eta\gg1$. Finally, although the final expression for the velocity is well defined at $\eta\to0$, to justify how close it is to the exact one (which is not

known) is an extremely difficult question. We shall not proceed further in this direction.

V. NUMERICAL RESULTS AND COMPARISON WITH EXPERIMENT

A. Numerical results

We now present some typical plots of the stationary velocity v_F vs the rescaled force $\tilde{F} \equiv F/\eta$ computed from (42). In Fig. 1 we present the dependence of the velocity curve on the magnitude of the quantum frequency Ω_q obtained from the $\eta \to 0$ limit of (42); the latter is well defined as long as we always rescale the force by $1/\eta$. This is similar to the behavior in the corresponding classical limit which can be analyzed by the Fokker-Planck equation.[8] Figure 1 shows that in the classical-like regime with $\Omega_q < 1$, the velocity rapidly approaches $\tilde{F}$, the stationary velocity in the absence of the cosine potential. The effects of the potential are thus mainly confined to the regime $\tilde{F} < 1$. However, as the quantum frequency increases the effects quickly extend to regimes well above $\tilde{F} = 1$. The striking feature here is that a wide plateau appears when $\Omega_q > 1$, which resembles a typical feature of the so-called Coulomb blockade discussed in the context of small Josephson junctions.[7,9]

The structure of the plateau is further examined in Fig. 2, where we plot its evolvement as a function of the temperature. At higher temperatures the height of the plateau is small. As the temperature decreases a broad peak appears near $\tilde{F} = \Omega_q/2$ with its height roughly equal to $\Omega_q/2$. As we lower the temperature further, a second peak appears at $\tilde{F} = 3\Omega_q/2$. Recall that in the absence of the periodic potential the free particle would move with a velocity $v_F = \Omega_q/2$ at $\tilde{F} = \Omega_q/2$. The energy of the particle is then $\hbar^2 k_0^2/8m$ [after restoring the dimension via (11)]. In k space it corresponds to the energy at the boundary of the first Brillouin zone. Similarly the next peak corresponds to the boundary of the third Brillouin zone. The physical reason for this structure is thus quite evident: When the particle moves close to the first Brillouin zone boundary, strong and coherent Bragg scattering occurs. The band structure of the Bloch states play a role now. The particle could either move into the next band or remain in the lowest band. As a result the stationary velocity of the particle shows a plateau or a peak at these positions, depending sensitively on the temperature. The second peak occurs when the first band and the second band come close again. Note that at higher temperatures our result indicates a smaller height of the plateau than that expected from the band-structure consideration. The plateau is more like a highly resistive state in terms of the I-V curve of a Josephson junction (cf. below). Figure 3 shows the effects of the viscosity on the plateau structure. We find that even a very small viscosity could cause rather considerable changes in v_F as $\tilde{F}$ becomes large. Raising the viscosity tends to destroy the quantum effects at lower values of $\tilde{F}$.

B. Comparison with experiment

We now discuss the relation of our result to the experimental observations in ultrasmall Josephson junctions summarized in Ref. 7. In a current-biased Josephson

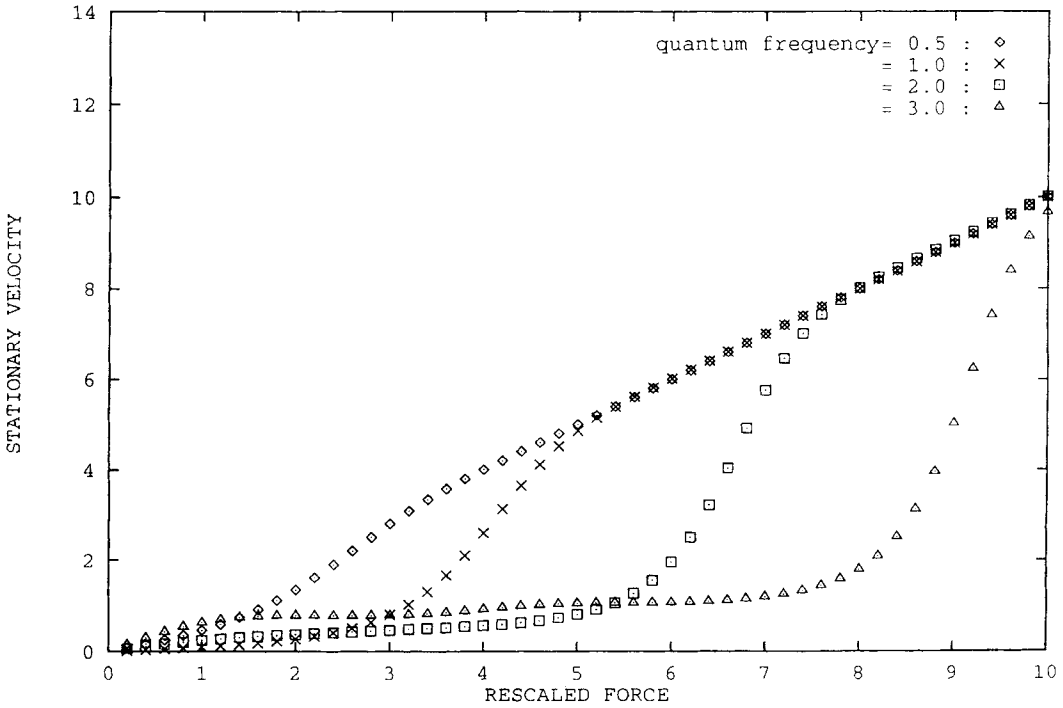

FIG. 1. Plots of the stationary velocity vs the rescaled force $\tilde{F} \equiv F/\eta$ for different quantum frequencies Ω_q at $T = 1.0$ and $\eta = 0$: ◇ for $\Omega_q = 0.5$, × for $\Omega_q = 1.0$, □ for $\Omega_q = 2.0$, and △ for $\Omega_q = 3.0$.

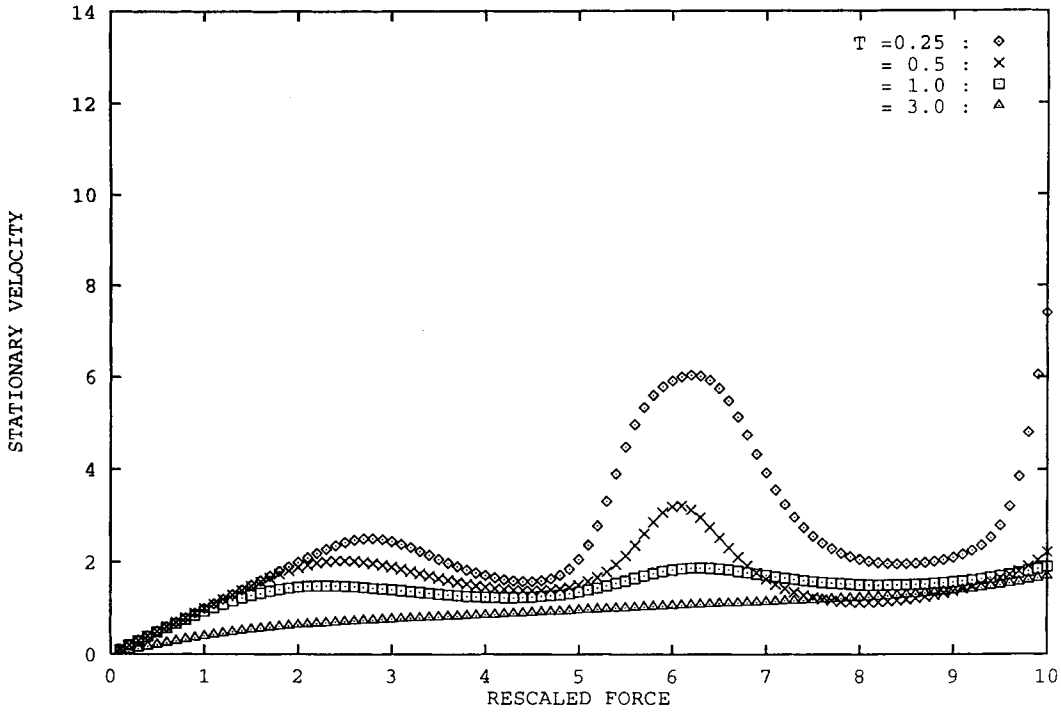

FIG. 2. The evolution of the plateau structure in terms of the temperature T for $\Omega_q=4.0$ and $\eta=0$: ◇ for $T=0.25$, × for $T=0.5$, □ for $T=1.0$,and △ for $T=3.0$. At higher temperature the curve becomes resistivelike.

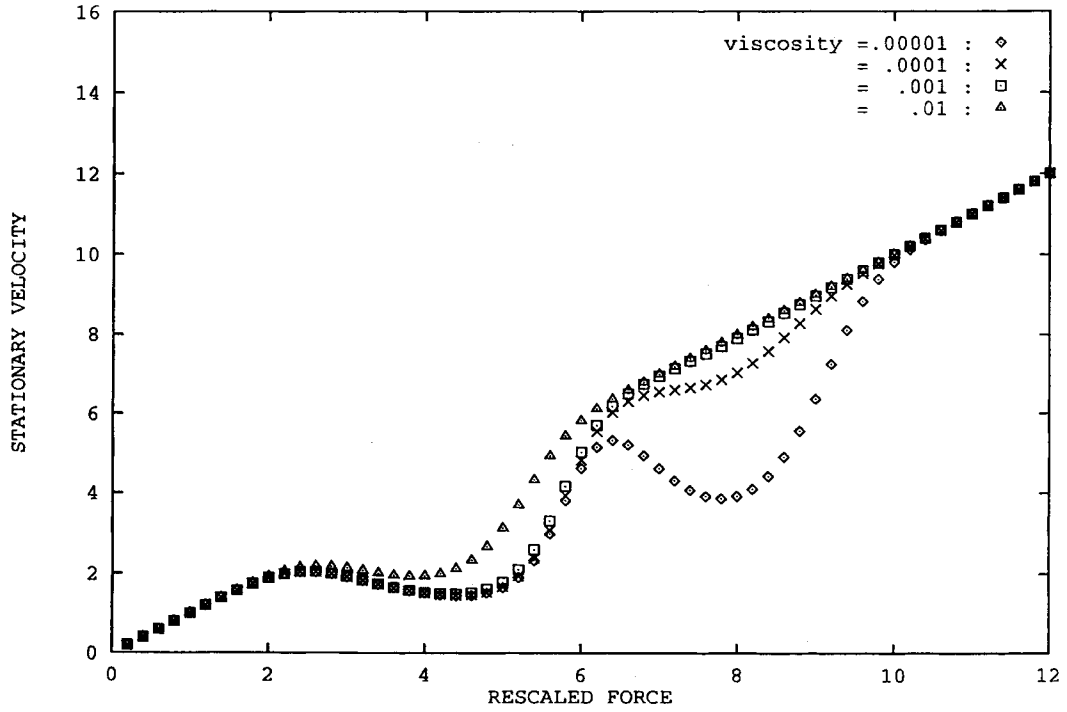

FIG. 3. The effects of the viscosity on the plateau structure for $\Omega_q=4.0$ and $T=0.5$: ◇ for $\eta=10^{-5}$, × for $\eta=10^{-4}$, □ for $\eta=10^{-3}$, and △ for $\eta=10^{-2}$. A larger viscosity causes the velocity to approach earlier to the value for the free motion.

junction, the intrinsic parameters of the system m, k_0, and V_0 are, respectively,

$$m=\left[\frac{\Phi_0}{2\pi}\right]^2 C\ ,\quad k_0\equiv 1\ ,\quad V_0=E_J=\frac{\Phi_0 I_c}{2\pi} \tag{47}$$

with $\Phi_0=h/2e$ the flux quantum, C the shunt capacitance, and I_c the critical current of the junction. The external driving force and the viscosity are proportional to, respectively, the bias current I and the inverse of the shunt resistance R (assuming the usual resistively shunted junction model); their dimensionless forms read

$$F=\frac{I}{I_c}\ ,\quad \eta=\left[\frac{\Phi_0}{2\pi I_c C R^2}\right]^{1/2}\ . \tag{48}$$

The dimensionless velocity v_F and quantum frequency Ω_q in this case are simply

$$v_F=V(C/E_J)^{1/2}\ ,\quad \Omega_q=\sqrt{2E_C/E_J} \tag{49}$$

with $E_C=e^2/2C$ being the Coulomb energy of the junction with a single electron charge. Note that because our calculation is based on a stationary-state formalism, it is expected to apply in the regimes where metastable states are irrelevant. We shall thus restrict our attention to the cases where the Josephson energy E_J, the Coulomb energy E_C, and the temperature are comparable with each other.

There are two basic features observed experimentally for the outgoing I-V characteristics in this regime: (a) When E_J and E_C are comparable, the metastable states of supercurrent with zero voltage disappears. They are replaced by a highly resistive I-V curve. (b) Further reducing E_J by applying a magnetic field results in a plateau at $V_b\cong e/2C$. The critical current $\tilde{I}_c$, now defined as the current at which the system makes a rapid switch to a much higher voltage state, is greatly reduced.

It is clear that the above features also appear in our analysis. In Fig. 1 both the resistive and the plateau states are present. Note that the curves are plotted with a fixed dimensionless temperature, while in the experiment, lowering E_J will result in raising both the dimensionless temperature and the quantum frequency. Therefore the possibility of mestable states at large E_J is not included in Fig. 1. The fact that the height of the plateau $\cong e^2/2C$ is also evident: The dimensionless velocity at $v_F\cong\Omega_q/2$ corresponds to, using the Josephson relation $V(t)=\dot{\phi}(t)\Phi_0/2\pi$, precisely the same dc voltage. It is thus natural to identify the observed critical current $\tilde{I}_c$ with the rather abrupt switches in the theoretical curves presented above. In Figs. 2 and 3, our analysis also indicates some subtle structures in the plateau regimes. At lower temperatures there are peaks representing the effects of the boundaries of the Brillouin zones. Nevertheless since the negative slope parts of an I-V curve should be unstable against fluctuations,[1] experimentally the system is expected to stay with a constant dc voltage in these regimes, making the I-V curves truly plateaulike. A jump is expected, however, if the second peak is substantially higher than the first one. This prediction remains to be tested by experiment.

To quantitatively fit the experimental data, one is forced to face several difficulties. Though the capacitance of an ultrasmall Josephson junction can now be determined with some accuracy from the height of the plateau, we find that the determination of the intrinsic critical current I_c (which is different from the observed one, $\tilde{I}_c$) is rather difficult (especially in the presence of the external magnetic field). The high nonlinearity of the quasiparticle damping also leads to uncertainties in, for example, what resistance is appropriate to the theory. Furthermore, the fact that the experiments seem to indicate rather sudden transitions at $\tilde{I}_c$, much sharper than that showed by our theoretical curves, may be related to the metastability and fluctuations in the system. Finally, if the present interpretation of the experiments is correct, some of the estimates of the junctions' parameters need to be reconsidered.

Despite these problems, let us nevertheless consider the best sample used in Ref. 7. The observed I-V curve is plotted in Fig. 3 of Ref. 7: it has $E_J=0.15$ K, i.e., the zero-field critical current $I_{c0}\cong 6.5$ nA (this estimate, obtained from the well-known Ambegaokar-Baratoff relation,[10] may, however, be too small, cf. below), $E_C=0.9$ K, $T=0.03$ K, and a leakage resistance $R_{L0}=3\times 10^8$ Ω. Letting the critical current in the presence of the magnetic field be $I_c(H)/I_{c0}=\gamma$, the dimensionless parameters would then be $T\cong 0.2/\gamma$, $\Omega_q\cong 3.5/\gamma^{1/2}$. Since the junction always has a finite voltage, the local temperature at the junction might be higher than 30 mK. We shall therefore also plot the theoretical I-V curve at 60 and 90 mK, i.e., $T\cong 0.4/\gamma$ and $T\cong 0.6/\gamma$. As one can see, raising temperature improves the agreement between theory and experiment.

We now describe the fitting process. To solve the problem of the nonlinear quasiparticle dissipation, we note that $\tilde{F}=F/\eta$ in our theory is nothing but the dimensionless velocity v_F^0 of the particle *in the absence of the Josephson potential.* It may thus be reasonable to identify it with the return part of the I-V curve which does not seem to be affected by the Josephson coupling (this is presumably due to the slow relaxation of the system into the truly stationary state). The very small but finite η here is also important. To be consistent with our solution for the nonlinear "free motion" we shall use $\eta=F/v_F^0$, which corresponds to the inverse of the nonlinear resistance at a given current, i.e., we use the η from the return curve as an input for the fitting.

We find, however, that for $\gamma\leq 1$ it is impossible to fit the experimental curve in any reasonable way. In fact $\gamma\cong 6$ seems to fit the curve best (cf. below for more discussions). The result is plotted in Fig. 4 for $T=30$ mK (in △), $T=60$ mK (in □), and $T=90$ mK (in ◇). The solid line there corresponds roughly to the observed outgoing I-V curve and the open line to the return curve. The predicted[11] $\tilde{I}_c$ is roughly $\tilde{I}_c^T\cong 4$–6 pA, which is still smaller than the observed one $\tilde{I}_c^E\cong 6.5$–7 pA. This may indicate that metastability plays some role at currents higher than $\tilde{I}_c^T$.

Finally let us address the question as why the

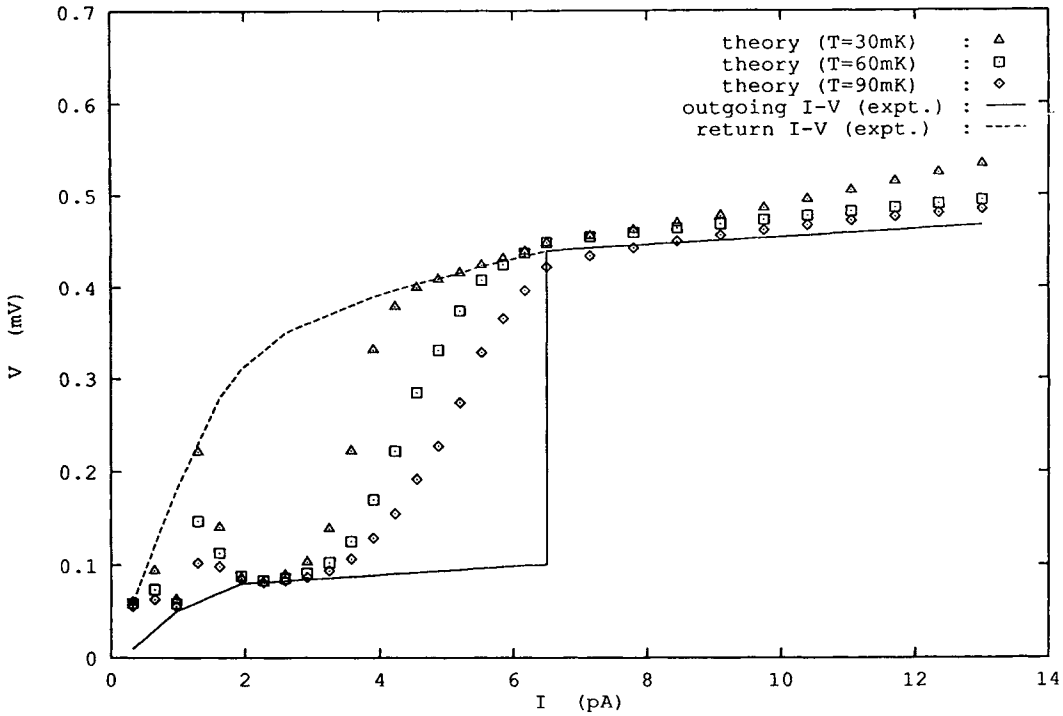

FIG. 4. Curves plotted in △ ($T=30$ mK), □ ($T=60$ mK), and ◇ ($T=90$ mK) are generated using the parameters inferred from Fig. 3 of Ref. 7 as discussed in the text. The actual experimental curves are represented roughly by the solid line for the outgoing I-V characteristic and the open line for the return one (the "free motion").

Ambegaokar-Baratoff relation, which relates the critical current I_{c0} to the above gap normal-state resistance R_n and the superconducting gap energy Δ via

$$I_{c0}=\frac{\pi\Delta}{2eR_n}\tanh\left[\frac{\Delta}{2kT}\right], \tag{50}$$

may not hold in this case. This relation is based on a microscopic tunneling Hamiltonian in which both normal electrons and Cooper pairs tunnel through the same barrier. While it seems to agree very well with a vast majority of measurements, its microscopic basis, i.e., the tunneling model in which $1/R_n \propto$ the square of the tunneling matrix element, becomes problematic when the Coulomb interaction between individual electrons near the tunneling barrier becomes important. The Coulomb blockade responsible for the observed plateau in the I-V curve may also greatly reduce the above-gap normal current, resulting in a considerable underestimate of the Josephson current.[12] In fact $\gamma \cong 6$ is consistent with other analyses in Ref. 7. In Eq. (9) of Ref. 7, I_{c0} should be multiplied by a factor of 7^2 while from Fig. 10 of Ref. 7 $I_c(H=0.2\text{ T})$ should be off by a factor of order 10. Furthermore, once I_c is reestimated, most of the other apparent fitting problems in Ref. 7 would disappear.

ACKNOWLEDGMENTS

This work was supported by the Youth Science Foundation of Basic Research, National Science Council of China and the U.S. Air Force Office of the Scientific Research through Grant No. 87-0010.

*Permanent address: Department of Physics, University of Science and Technology of China, Hefei, Anhui 230026, China.

[1]Y.-C. Chen, M. P. A. Fisher, and A. J. Leggett, J. Appl. Phys. **64**, 3119 (1988).

[2]Y.-C. Chen, J. L. Lebowitz, and C. Liverani, Phys. Rev. B **40**, 4664 (1989); Y.-C. Chen, J. Stat. Phys. **65**, 761 (1991).

[3]Y.-C. Chen and J. L. Lebowitz, preceding paper, Phys. Rev. B **46**, 10 743 (1992).

[4]U. Weiss, M. Sassetti, T. Negele, and M. Wollensak, Z. Phys. B **84**, 471 (1991); U. Weiss and M. Wollensak, Phys. Rev. B **37**, 2729 (1988).

[5]W. Zwerger, Phys. Rev. B **35**, 4737 (1987).

[6]For a general review and references, see P. Hänggi, P. Talkner, and M. Borkovec, Rev. Mod. Phys. **62**, 251 (1990).

[7]M. Iansiti, M. Tinkham, A. T. Johnson, W. F. Smith, and C. J. Lobb, Phys. Rev. B **39**, 6465 (1989), and references therein.

[8]H. Risken, *The Fokker-Planck Equation* (Springer-Verlag, Berlin, 1984), Chap. 11.

[9]D. V. Averin and K. K. Likharev, J. Low Temp. Phys. **62**, 345 (1986); for a recent review, see G. Schön and A. D. Zaikin, Phys. Rep. **198**, 237 (1990).

[10]V. Ambegaokar and A. Baratoff, Phys. Rev. Lett. **10**, 486 (1963).

[11]The identification of the theoretical turning point is rather

vague. The problem here is similar to the classical one using the Fokker-Planck equation: it is difficult to judge from a calculation based on a stationary distribution where the system is to jump out of a metastable state. See Ref. 8.

[12]The question why the Coulomb blockade is less significant for the supercurrent remains to be studied. It is probably due to the coherence of the Cooper pairs, cf. also Ref. 9.